Journal of Power Sources 195 (2010) 6108–6115

Contents lists available at ScienceDirect

Journal of Power Sources

journal homepage: www.elsevier.com/locate/jpowsour

The electrochemical property of ZrF_x-coated $Li[Ni_{1/3}Co_{1/3}Mn_{1/3}]O_2$ cathode material

Su Hyun Yun [a], Kyu-Sung Park [b], Yong Joon Park [a,*]

[a] Department of Advanced Materials Engineering, Kyonggi University, San 94-6, Yiui-dong, Yeongtong-gu, Suwon, Gyeonggi-do 443-760, Republic of Korea
[b] Battery Group, Samsung Advanced Institute of Technology (SAIT), Yongin 446-712, Republic of Korea

ARTICLE INFO

Article history:
Received 30 September 2009
Received in revised form 3 November 2009
Accepted 3 November 2009
Available online 13 November 2009

Keywords:
Surface coating
Electrochemical property
Cathode
Lithium battery

ABSTRACT

Electrochemical and thermal properties of pristine and ZrF_x-coated $Li[Ni_{1/3}Co_{1/3}Mn_{1/3}]O_2$ cathode materials are compared. The hydrothermal method is introduced for the fabrication of a uniform coating layer. The formation of a compact coating layer on the surface of pristine powder is observed by scanning electron microscopy (SEM) and transmission electron microscopy (TEM). From TEM–EDS and XPS analysis, it is inferred that the coating layer is ZrO_xF_y (zirconium oxyfluoride) form. The coated $Li[Ni_{1/3}Co_{1/3}Mn_{1/3}]O_2$ electrodes have better rate capability and cyclic performance at high temperature compared with the pristine electrode. The thermal stability of the $Li[Ni_{1/3}Co_{1/3}Mn_{1/3}]O_2$ electrode is also enhanced by the ZrF_x coating. Such enhancements are due to the presence of a stable coating layer, which effectively suppresses the chemical instability ascribed to surface reaction between electrode and electrolyte.

1. Introduction

Lithium ion batteries were commercialized in 1991 and their use as power sources for portable electronic devices, especially cellular phones and laptop computers, has increased in past years. Recently, much effort has focused on developing a large-scale lithium ion battery for use in electric vehicles (EVs), hybrid electric vehicles (HEVs) and plug-in hybrid electric vehicles (PHEVs) [1–4]. Most commercial lithium ion batteries for portable devices use $LiCoO_2$ as the cathode material. However, because of the small capacity and high cost of $LiCoO_2$, extensive research has been carried out to find an alternative cathode material that offers lower cost and higher capacity. $Li[Ni_{1/3}Co_{1/3}Mn_{1/3}]O_2$ is one of the most promising new cathode materials since its electrochemical property is comparable or superior to the properties of other alternative cathode materials [5–11]. However, to meet the challenging requirements of new applications such as usage in EV, HEV and PHEV, $Li[Ni_{1/3}Co_{1/3}Mn_{1/3}]O_2$ needs to be improved in terms of power density, safety, and cyclic performance.

Surface coating has been investigated as a method to improve the battery performances. As coating materials, oxides [12–18] and phosphates [19–22] have been suggested for enhancing electrochemical properties. Surface coating has resulted in reduced cation dissolution during cycling, lower impedance resistance of the interface between cathode and electrolyte, and enhanced structural stability at high voltage. However the coating effect of cathodes is highly attributable to the specific coating material [18,19]. Some coating materials are very effective in improving electrochemical and other properties, whereas others are not. Therefore, introduction of a suitable coating material is a key factor in obtaining a highly improved cathode material via surface coating. In this paper, zirconium fluoride (ZrF_x) is introduced as a coating material for the $Li[Ni_{1/3}Co_{1/3}Mn_{1/3}]O_2$ cathode for the first time. Zr is an effective coating substituent in the form of zirconium oxide [23–25]. F was investigated as a doping material for enhanced structural and thermal stability [26–28], and some fluorides such as AlF_3 were successfully used as a surface coating material for improved electrochemical properties [29–31]. Zirconium fluoride have been used as fluoride glass [32–34] or surface coating for alloy metals [35] due to their chemical stability, but it has not been introduced as surface coating material for cathode of lithium battery. In this study, we fabricate a $Li[Ni_{1/3}Co_{1/3}Mn_{1/3}]O_2$ cathode that is surface modified with ZrF_x, and examine the electrochemical and structural properties of the coated electrode. In particular, the hydrothermal method for coating is adopted to achieve a more uniform coating. Generally, the process of coating is conducted by mixing cathode powders and coating solution and then drying and heat treating (hereafter, referred as the 'wet process'). However, the hydrothermal method employing temperature and pressure to react the cathode and coating solution can achieve a more uniform coating on the surface of a pristine cathode. Thus, it is expected that the uniform coating layer produced via the hydrothermal method will offer better coating effects such as an improved rate capability.

* Corresponding author. Tel.: +82 31 249 9769.
E-mail addresses: yjpark2006@kyonggi.ac.kr, yjparketri@yahoo.co.kr (Y.J. Park).

0378-7753/$ – see front matter © 2009 Elsevier B.V. All rights reserved.
doi:10.1016/j.jpowsour.2009.11.022

2. Experimental

Pristine $Li[Ni_{1/3}Co_{1/3}Mn_{1/3}]O_2$ powder was supplied by ECO-PRO. The ZrF_x coating was prepared using the hydrothermal method. First, Zr $(CH_3CO_2)_2{\cdot}(OH)_2$ (99.99%, Aldrich) and NH_4F(98%+, Aldrich) were dissolved in distilled water, and the solution was stirred continuously for 2 h at 25 °C. The molar ratio of the Zr source to the F source was adjusted to 1:4 (assumed ZrF_4). Subsequently, $Li[Ni_{1/3}Co_{1/3}Mn_{1/3}]O_2$ powder was added to the coating solution and mixed thoroughly for 1 h at 25 °C. The slurry containing mixed powder was transferred to a Teflon-sealed stainless-steel autoclave and sealed tightly. The autoclave was heated to 120 °C and the temperature maintained for 15 h to promote the hydrothermal reaction. In addition, the slurry was dried in an oven at 100 °C for 12 h and heat treated in a furnace at 400 °C for 5 h under air. A coated sample prepared using the typical wet process was also fabricated to compare with that prepared using the hydrothermal method. The same coating solution mentioned above was mixed with $Li[Ni_{1/3}Co_{1/3}Mn_{1/3}]O_2$ powder and stirred at 80 °C for 2 h and dried in an oven at 100 °C for 12 h. Samples were the heat treated in a furnace at 400 °C for 5 h under air.

The pristine sample was also heat treated at 400 °C for 5 h before electrochemical test to prevent from the heating effect on the electrochemical property of the cathode powder. The microstructure of the powder was observed by field-emission scanning electron microscopy (FE-SEM, JEOL-JSM 6500F). A cross section polisher (SM-0901, JEOL) and field-emission scanning electron microscopy (FE-SEM, JSM-7000F, JEOL) were employed to investigate the cross-sectional image of the powder. X-ray photoelectron spectroscopy (XPS, Quantum 2000 Scanning ESCA Microprobe, Physical Electronics) was performed to compare the compositions and ionic environments of pristine and coated samples using f used monochromatized Al Kα radiation (1486.6 eV). The residual pressure inside the analysis chamber was 7×10^{-9} Torr. Transmission electron microscopy (TEM, JEOL-JEM 2100F) was also carried out using an electron microscope, operating at 200 kV.

The electrochemical performance of the coated $Li[Ni_{1/3}Co_{1/3}Mn_{1/3}]O_2$ cathodes was examined using two-electrode test cells (of 2032 configuration) consisting of a cathode, metallic lithium anode, polypropylene separator, and an electrolyte of 1 M LiPF6 in EC/DMC (1:1 vol.%). The cathode contained 80 wt.% active materials, 12 wt.% carbon black, and 8 wt.% PVDF binder. The components were ball-milled for homogeneous mixing and then coated on aluminum foils and dried at 90 °C for 2 h. The cells were assembled in an Ar-filled glove box. Cells were subjected to galvanostatic cycling using a WonAtech (WBCS 3000) charge–discharge system. DSC (differential scanning calorimetry) samples for the cathode were prepared by the following treatment before testing. The cells containing sample electrodes were charged to 4.6 or 4.8 V at a current density of 0.2*C*, and the potential was held until the current density reached 4 mA g^{-1}. The cells were then disassembled in a dry room to remove the charged positive electrode. A 5 mg of the positive electrode containing electrolyte was sealed in a high-pressure DSC pan. The heating rate and temperature range in the DSC tests were 5 °C min^{-1} and 25–350 °C, respectively.

3. Results and discussion

The surfaces of pristine and ZrF_x-coated $Li[Ni_{1/3}Co_{1/3}Mn_{1/3}]O_2$ were observed by scanning electron microscopy (SEM), as shown in Fig. 1. The pristine powder consisted of polyhedral primary particles (0.2–0.5 μm in size). The insets show the circular shapes of the powders. The surface morphology of the pristine sample was smooth and clean without any heterophase particles. On the other hand, the surfaces of coated samples were rough and covered with nanoparticles, which appeared to be the coating layers. As the percentage weight of the coating material increased, the

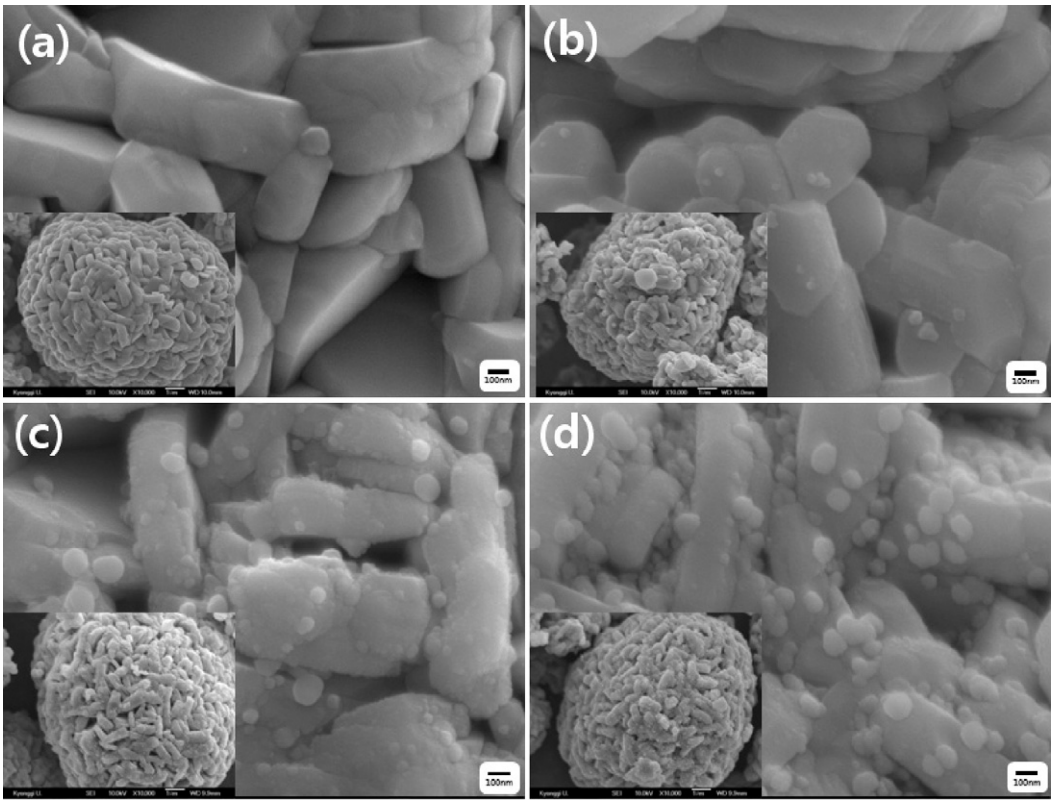

Fig. 1. SEM images of (a) pristine and (b) 0.25 wt.%, (c) 0.5 wt.%, (d) 1.0 wt.% ZrF_x-coated $Li[Ni_{1/3}Co_{1/3}Mn_{1/3}]O_2$ powders.

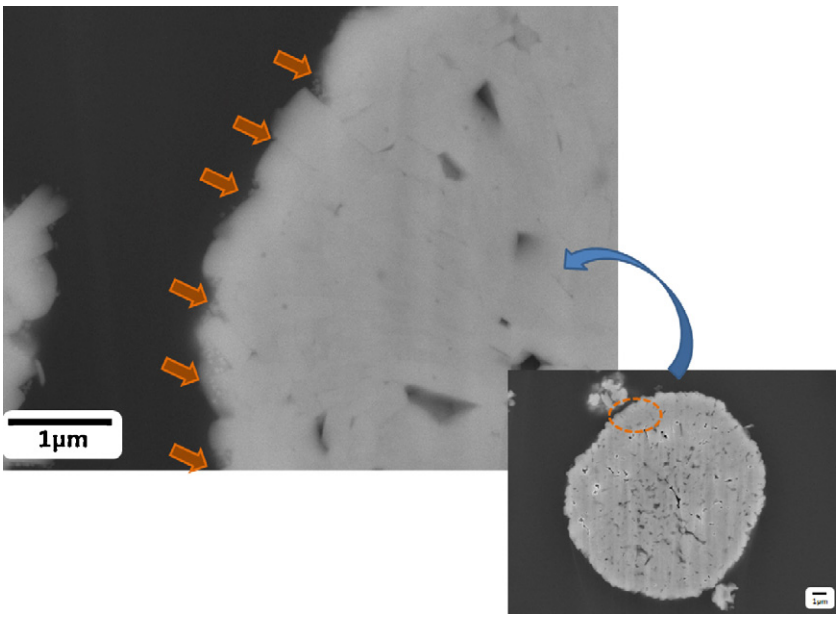

Fig. 2. Cross-sectional SEM images of 1.0 wt.% ZrF_x-coated $Li[Ni_{1/3}Co_{1/3}Mn_{1/3}]O_2$ powder.

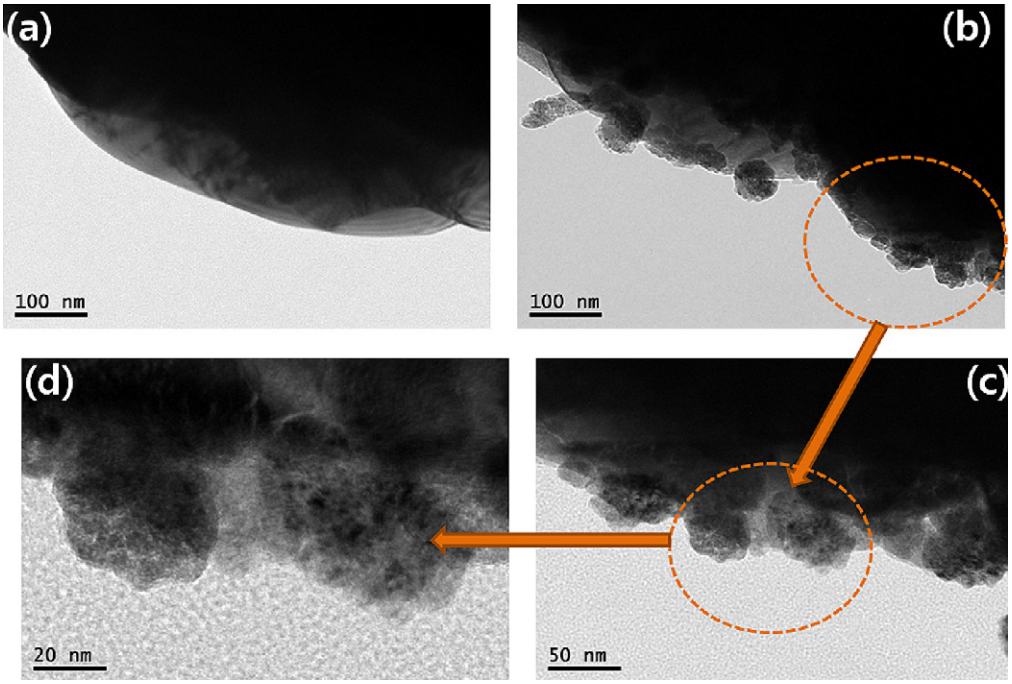

Fig. 3. TEM images of (a) pristine $Li[Ni_{1/3}Co_{1/3}Mn_{1/3}]O_2$ powder and (b) 1.0 wt.% ZrF_x-coated $Li[Ni_{1/3}Co_{1/3}Mn_{1/3}]O_2$ powder; (c) magnified image of (b); (d) magnified image of (c).

Table 1
Discharge capacity and capacity retention of $Li[Ni_{1/3}Co_{1/3}Mn_{1/3}]O_2$ samples at various *C* rates (values of the first cycle). Percentages refer to the capacity retention compared with the discharge capacity at the 1*C* rate.

	Pristine (mAh g^{-1})	Pristine (%)	ZrF_x0.25 wt.% (mAh g^{-1})	ZrF_x0.25 wt.% (%)	ZrF_x0.5 wt.% (mAh g^{-1})	ZrF_x0.5 wt.% (%)	ZrF_x1.0 wt.% (mAh g^{-1})	ZrF_x1.0 wt.% (%)
1*C*	170.52	100.0	174.33	100.0	176.96	100.0	175.93	100.0
2*C*	148.45	87.1	154.61	88.7	160.58	90.7	161.44	91.8
4*C*	118.32	69.4	128.31	73.6	136.93	77.4	138.21	78.6
6*C*	89.28	52.4	100.11	57.4	116.54	65.9	116.70	66.3
8*C*	57.72	33.8	66.00	37.9	95.15	53.8	93.84	53.3
10*C*	25.43	14.9	30.73	17.6	70.57	39.9	68.46	38.9
12*C*	7.82	4.6	8.54	4.9	44.03	24.9	43.97	25.0

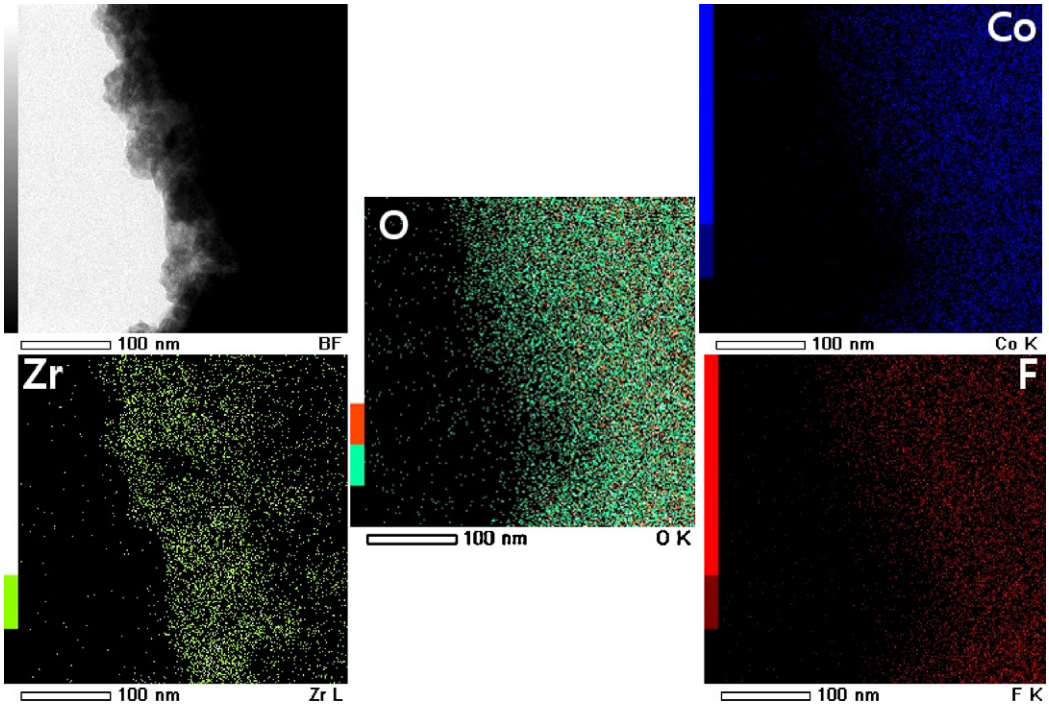

Fig. 4. TEM mapping images of 1.0 wt.% ZrF_x-coated $Li[Ni_{1/3}Co_{1/3}Mn_{1/3}]O_2$ powder.

number of surface nanoparticles increased obviously in the SEM images. However, the size of nanoparticles was not affected by the amount of coating material. The nanoparticles had very uniform size of ~50 nm. Fig. 2 shows the cross-sectional SEM image of ZrF_x-coated (1 wt.%) $Li[Ni_{1/3}Co_{1/3}Mn_{1/3}]O_2$ powder. The arrows indicate the nanoparticles adhering to the surface of the pristine powder. The coating material is likely to diffuse easily into the surface and react with elements of the bare material such as Li, Co, Ni, and Mn because of the high surface free energy of nanoparticles, which is attributed to their size. Therefore, it is difficult to distinguish the exact coating layer from the powder and analyze the exact composition of the coating layer.

To investigate the surface morphology of pristine and coated samples in detail, TEM analysis was performed. As shown in Fig. 3, the pristine particles had a smooth surface, whereas the surfaces of coated $Li[Ni_{1/3}Co_{1/3}Mn_{1/3}]O_2$ particles were covered with a coating layer. The coated particles seemed to be circular, and uniformly distributed on the surface of the pristine powder. Fig. 4 shows the element mapping result obtained by the TEM–energy dispersive spectrometry (EDS) system. The spot intensity is an indicator of the element or concentration. The denser the spot accumulation, the higher the spot content. Dense Zr EDS spots on the surface of the powder indicate that most Zr content accumulated in the coating layer and vicinity of coating particles. Co EDS spots were uniformly distributed in the powder, except in the surface layer. Contrary to our expectation, F EDS spots were scattered in the interior of the powder as well as in the coating layer. This indicates that F diffused into the powder during heat treatment. Likewise, the O EDS spots were observed not only within the powder but also in the coating layer. However the less dense O EDS spots in the coating layer indicate that the coating layer is not composed of just the zirconium oxide form. EDS analysis infers that the coating material loses a bit of F and reacts with oxygen on the surface of pristine powder, so the real composition of the coating layer may be the ZrO_xF_y (zirconium oxyfluoride) form. Although F does not perfectly accumulate on the coating layer, the doped F can contribute to the enhancing of properties such as the thermal stability [26–28]. The surface composition was also characterized by X-ray photoelectron spectroscopy (XPS). Fig. 5 shows the XPS spectra of pristine and surface modified (1 wt.%) $Li[Ni_{1/3}Co_{1/3}Mn_{1/3}]O_2$ particles. Zr 3d and F 1s peaks were detected for the coated sample. The binding energies of Zr 3d and F 1s were 182.4 and 685.3 eV, respectively. Both pristine and coated samples had Co 2p, Ni 2p, and Mn 2p peaks without remarkable chemical shift of the binding energy, indicating that the Co, Ni, and Mn ion environment in the structure did not change. However, it is clear that the intensities of the peaks were decreased by the coating, which is likely due to the formation of a ZrF_x coating. In contrast, the shape of O 1s spectra was little changed. The small chemical shift of the binding energy of O 1s implies that the oxygen environment of the $Li[Ni_{1/3}Co_{1/3}Mn_{1/3}]O_2$ structure was not significantly altered by the surface coating. The lower intensities of the O 1s peaks for the coated samples imply that some of the fluoride formed on the surface was replaced by an oxide layer. The small and broad peak located at 531–532 eV in the pristine spectra is likely due to impurities with OH^- or O^- bonding on the surface. It was not present after the coating treatment. On the surface layer, small amounts of impurities could be formed via an unwanted reaction with oxygen or moisture in the air. The coating consists of nanoparticles with high surface energy that can easily react with surface impurities and remove the unstable surface layer, which may improve the electrochemical property of the electrode.

The electrochemical properties of pristine and coated $Li[Ni_{1/3}Co_{1/3}Mn_{1/3}]O_2$ electrode were characterized to investigate the coating effect on capacity, cyclic performance and rate capability. Fig. 6 shows the discharge capacities and cyclic properties of the pristine and coated $Li[Ni_{1/3}Co_{1/3}Mn_{1/3}]O_2$ electrodes at 1, 2, 4, 6, 8, 10, and 12*C* rates in the voltage range of 4.6–3.0 V. Coated samples had discharge capacities similar to or a slightly greater than that of the pristine sample at a 1*C* rate. However, at high *C* rates, coated samples had remarkably superior discharge capacity compared with the capacity of the pristine sample. Fig. 7 shows initial discharge profiles of pristine and ZrF_x-coated $Li[Ni_{1/3}Co_{1/3}Mn_{1/3}]O_2$ electrodes at 2, 6, and 12*C* rates. The coated samples had higher discharge capacity at all *C* rates. This indicates that use of a ZrF_x coating is effective in achieving

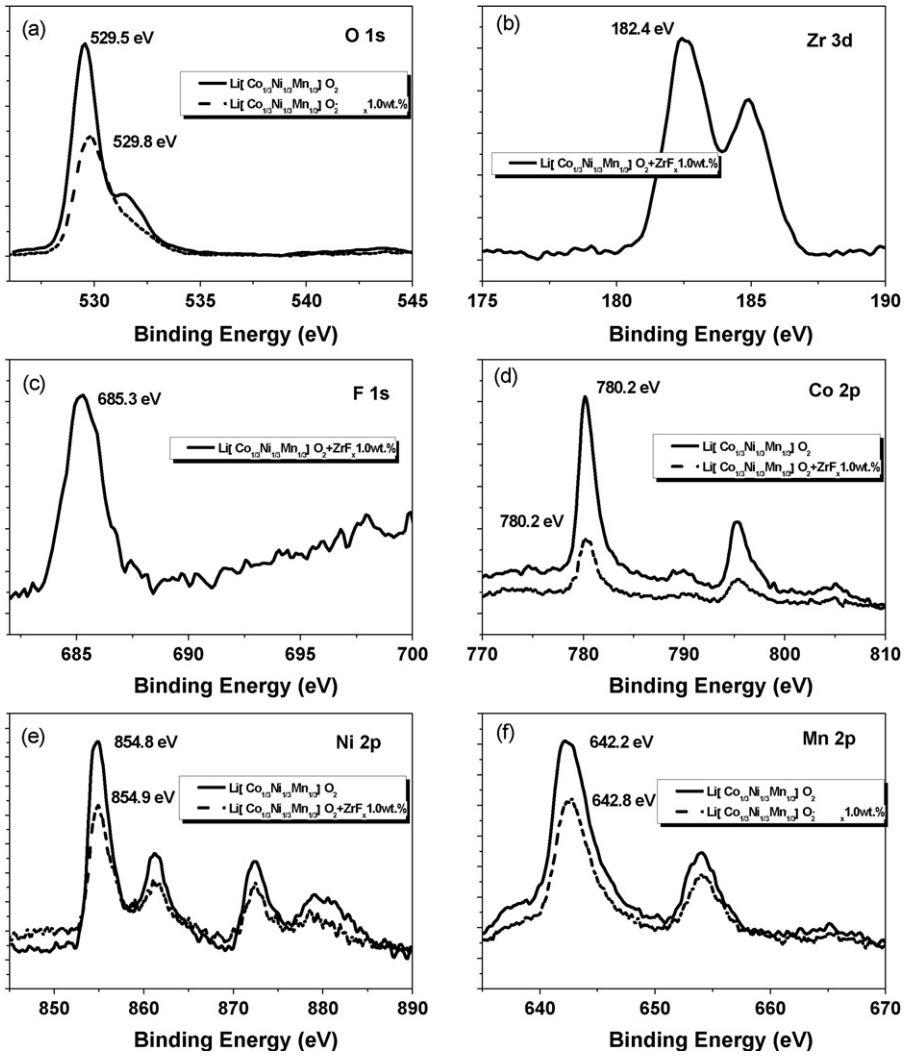

Fig. 5. XPS spectra of pristine and 1.0 wt% ZrF_x-coated $Li[Ni_{1/3}Co_{1/3}Mn_{1/3}]O_2$ cathode. (a) O 1s; (b) Zr 3d; (c) F 1s; (d) Co 2p; (e) Ni 2p and (f) Mn 2p.

an enhanced rate capability for the cathode material. In particular, the 0.5 and 1 wt.% coated samples had a better rate capability than the 0.25 wt.% coated sample did. Fig. 8 displays the capacity retention (ratio of the discharge capacity at an assigned *C* rate to the discharge capacity at a 1*C* rate) as a function of the *C* rate, which was measured during continuous cycling at respective *C* rates. Capacity retentions at 10 and 12*C* rates compared with the 1*C* rate were only ~15% and ~5%, respectively, for the pristine sample. However 0.5 and 1 wt.% coated samples had ~39% (10*C* rate) and ~25% (12*C* rate) capacity retention under the same measurement conditions. Table 1 summarizes the discharge capacity and capacity retention at various *C* rates (the values of the initial cycle at respective *C* rates). The enhanced rate capability due to surface coating is a similar result to that previously reported [12,18–22]. The surface of the cathode, which is in direct contact with the liquid electrolyte, is vulnerable. The HF in the electrolyte, which is produced via the decomposition of $LiPF_6$ salt, attacks the surface of the cathode, and thus the transition metals (Co, Ni, and Mn ions) of the cathode structure dissolve into the electrolyte, and an interface layer, which interrupts the diffusion of lithium ions and electrons, forms on the surface of the cathode [12,18]. The vulnerable surface of the electrode could be protected by a surface coating. The stable surface film layer can reduce transition metal dissolution and suppress the formation of an unwanted surface layer, which leads to an enhanced rate capability of the coated cathode. A 0.25 wt.% coating of ZrF_x is not enough to obtain a sufficient coating effect, and thus a coating in excess of 0.5 wt.% is needed to improve the rate capability of the $Li[Ni_{1/3}Co_{1/3}Mn_{1/3}]O_2$ electrode.

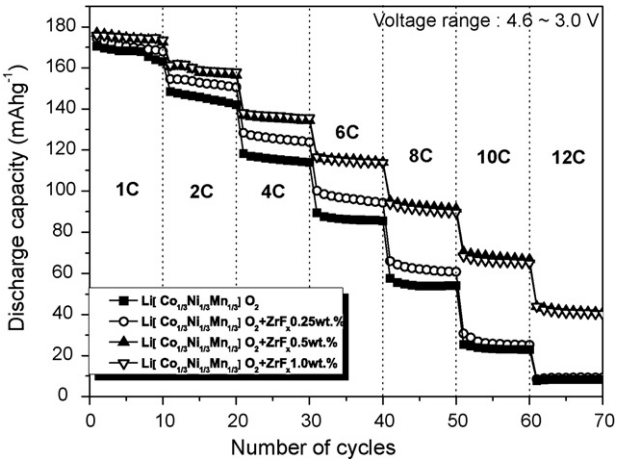

Fig. 6. Discharge capacities and cyclic performances of pristine and coated $Li[Ni_{1/3}Co_{1/3}Mn_{1/3}]O_2$ electrodes in the voltage range of 4.6–3.0 V at 1, 2, 4, 6, 8, and 12*C* rates.

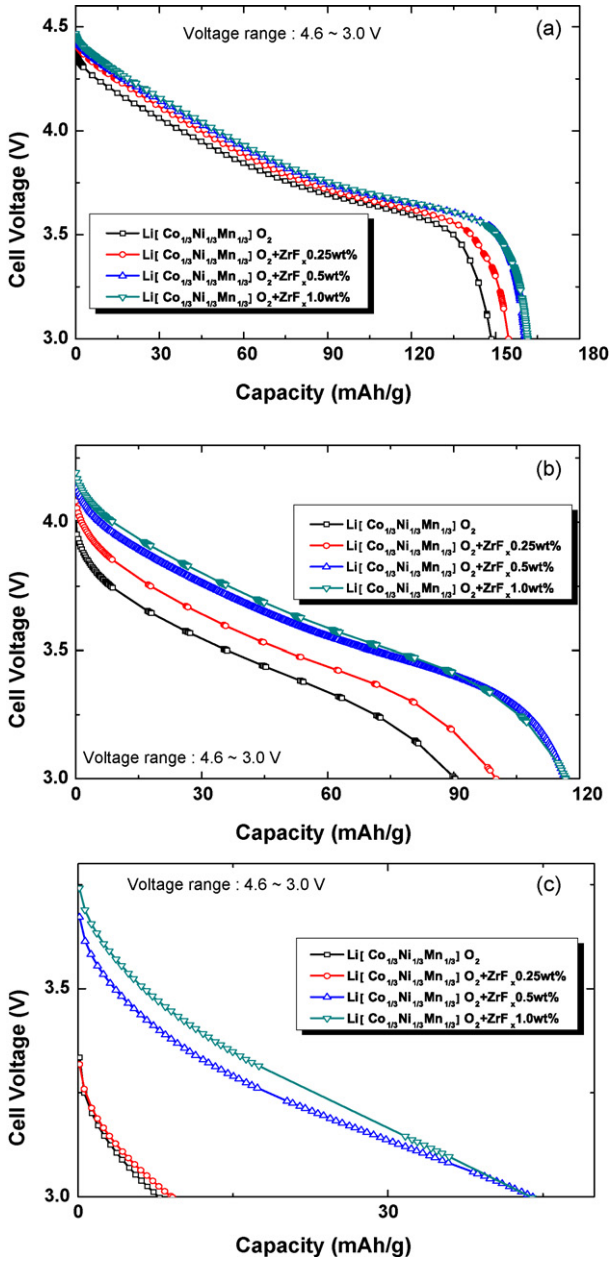

Fig. 7. Initial discharge profiles of pristine and ZrF_x-coated $Li[Ni_{1/3}Co_{1/3}Mn_{1/3}]O_2$ electrodes in the voltage range of 4.6–3.0 V at (a) 2*C*, (b) 6*C*, and (c) 12*C* rates.

To demonstrate the effect of the hydrothermal coating, the general wet process was also employed to produce a ZrF_x coating. Fig. 9 presents the discharge capacities and rate capabilities of pristine and 1 wt.% ZrF_x-coated $Li[Ni_{1/3}Co_{1/3}Mn_{1/3}]O_2$ electrodes, prepared by the hydrothermal method and wet process, at different *C* rates. Coated samples produced using either method had higher discharge capacity and better rate capability than the pristine sample. However, the sample coated using the hydrothermal method had obviously superior rate capability than the sample coated using the wet process. It was difficult to verify by SEM or TEM images, most of the coated powders prepared using the hydrothermal method had a uniform coating. In contrast, no complete coating layer was observed for some coated powder prepared using the typical wet process in SEM, although a large portion of the powder was coated sufficiently. This confirms the assumption that the use of the hydrothermal method is beneficial in preparing a uniform surface coating because

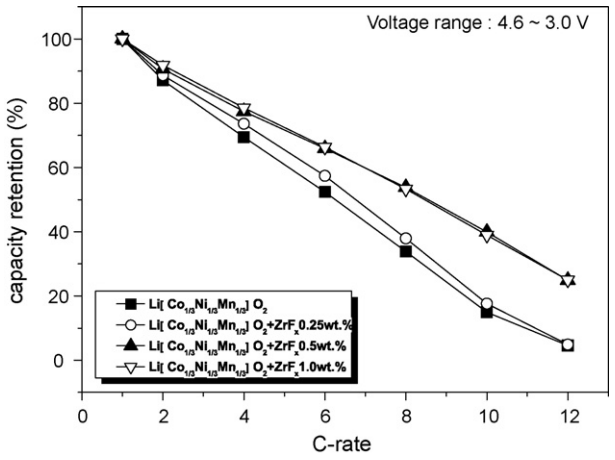

Fig. 8. Capacity retentions of pristine and coated $Li[Ni_{1/3}Co_{1/3}Mn_{1/3}]O_2$ electrodes as functions of *C* rates.

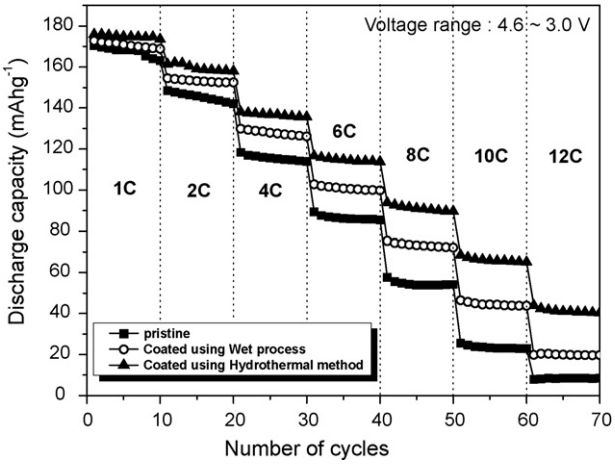

Fig. 9. Comparison of discharge capacities and rate capabilities of pristine and coated $Li[Ni_{1/3}Co_{1/3}Mn_{1/3}]O_2$ electrodes in the voltage range of 4.6–3.0 V at 1, 2, 4, 6, 8, and 12*C* rates.

heat and pressure facilitate the reaction between coating nanoparticles and the surface of pristine powder. Therefore the superior electrochemical properties of coated samples produced using the hydrothermal method are likely due to the more uniform coating.

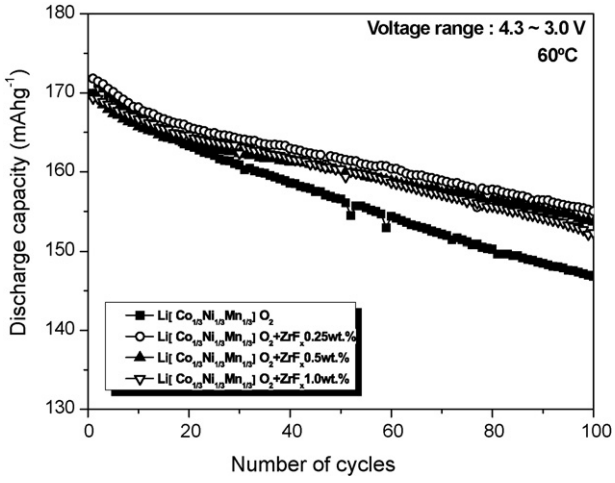

Fig. 10. Cyclic performances of pristine and ZrF_x-coated $Li[Ni_{1/3}Co_{1/3}Mn_{1/3}]O_2$ electrodes in the voltage range of 4.3–3.0 V at 60 °C (1*C* rate).

Table 2
Discharge capacities and capacity retentions of pristine and ZrF_x-coated $Li[Ni_{1/3}Co_{1/3}Mn_{1/3}]O_2$ electrodes during 100 cycles in the voltage range of 4.3–3.0 V at 60 °C. Percentages refer to the capacity retention during 100 cycles.

	Pristine ($mAh\,g^{-1}$)	Pristine (%)	ZrF_x0.25 wt.% ($mAh\,g^{-1}$)	ZrF_x0.25 wt.% (%)	ZrF_x0.5 wt.% ($mAh\,g^{-1}$)	ZrF_x0.5 wt.% (%)	ZrF_x1.0 wt.% ($mAh\,g^{-1}$)	ZrF_x1.0 wt.% (%)
1st	169.96	86.4	171.81	90.2	169.73	90.5	169.31	89.9
100th	146.83		155.01		153.65		152.29	

The coating effect on the cyclic performance of the $Li[Ni_{1/3}Co_{1/3}Mn_{1/3}]O_2$ electrode was characterized under a harsh cycling condition. Both pristine and coated $Li[Ni_{1/3}Co_{1/3}Mn_{1/3}]O_2$ electrodes had stable cyclic performance at room temperature, as shown in Fig. 6. To examine the effect of the ZrF_x coating on the cycling behavior under a chemically unstable condition, the temperature of the measuring chamber was increased to 60 °C. To avoid the effect of electrolyte decomposition at high voltage under high temperature, the upper cut-off voltage was reduced to 4.3 V. Fig. 10 displays the cyclic performance of pristine and coated $Li[Ni_{1/3}Co_{1/3}Mn_{1/3}]O_2$ electrodes in the voltage range of 4.3–3.0 V at 60 °C. The discharge capacity of the pristine sample rapidly dropped during cycling. However, the coated sample clearly had improved cyclic behavior, which indicates that ZrF_x coating is also effective in achieving greater chemical stability for $Li[Ni_{1/3}Co_{1/3}Mn_{1/3}]O_2$ at high temperature. Table 2 summarizes the discharge capacity before and after 100 cycles and the capacity retention of pristine and coated $Li[Ni_{1/3}Co_{1/3}Mn_{1/3}]O_2$ electrodes. The capacity retention of the pristine electrode during 100 cycles was 86.4%. However, the capacity retention increased to 90.2%, 90.5%, and 89.9% for the 0.25, 0.5, and 1.0 wt.% coated samples, respectively. The capacity fading was not perfectly suppressed, but the rapid loss of capacity by chemical reaction between electrode and electrolyte at high temperature was reduced by the surface coating.

In the following test, the thermal stability of the $Li[Ni_{1/3}Co_{1/3}Mn_{1/3}]O_2$ electrode before and after coating was investigated using DSC analysis. The electrodes were charged to 4.6 or 4.8 V before the test and sealed in a high-pressure DSC pan. Fig. 11 presents the DSC profile of the pristine and 1 wt.% coated $Li[Ni_{1/3}Co_{1/3}Mn_{1/3}]O_2$ electrodes. For the pristine sample charged to 4.6 V, thermal reaction with the electrolyte commenced at roughly ~180 °C and heat was generated until ~300 °C. There were two exothermic peaks at low temperature (180–250 °C), and a large peak at ~288 °C, as shown in Fig. 11a. The amounts of heat generation for the two exothermic regions were 628 and 595 $J\,g^{-1}$, respectively. The DSC spectrum of the pristine sample charged to 4.8 V had a similar shape to that of the sample charged to 4.6 V. The large exothermic peak shifted to lower temperature (~264 °C) and heat generation of that region increased a little to 610 $J\,g^{-1}$. However, the amount of heat generation at the low temperature (180–240 °C) decreased to 340 $J\,g^{-1}$. As shown in Fig. 11c and d, the amount of heat generation was decreased by the ZrF_x surface coating. In the spectrum of the coated sample charged to 4.6 V, the exothermic peak at low temperature (170–270 °C) had a broad shape, and heat generation dropped to 340 $J\,g^{-1}$. The large peak in the high temperature region shifted to 293 °C, but the heat generation increased a little. The effect of the coating on thermal stability was more prominent in the DSC profile of the coated sample charged to 4.8 V. The peaks in the temperature range of 180–250 °C almost vanished and heat generation of the large exothermic peak at 264 °C dramatically decreased to 119 $J\,g^{-1}$, indicating significant enhancement of the thermal stability of the $Li[Ni_{1/3}Co_{1/3}Mn_{1/3}]O_2$ electrode. This enhancement may be ascribed to the suppression of the surface reaction between electrode and electrolyte in a fully charged state by the stable ZrF_x coating.

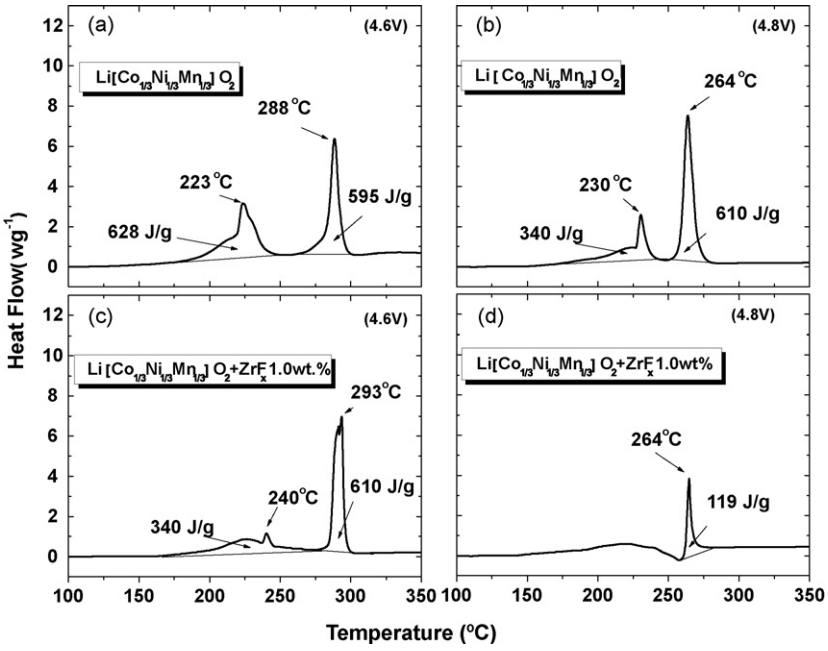

Fig. 11. DSC profiles of the $Li[Ni_{1/3}Co_{1/3}Mn_{1/3}]O_2$ electrode. (a) Pristine sample charged to 4.6 V; (b) pristine sample charged to 4.8 V; (c) 1.0 wt.% coated sample charged to 4.6 V and (d) 1.0 wt.% coated sample charged to 4.8 V.

4. Conclusions

$Li[Ni_{1/3}Co_{1/3}Mn_{1/3}]O_2$ cathode material was successfully coated with ZrF_x. SEM and TEM images confirmed that ZrF_x formed as a compact coating over the cathode particles. On the basis of the results of TEM–EDS, it could be inferred that the composition of the coating layer was in ZrO_xF_y (zirconium oxyfluoride) form. In the XPS analysis of pristine and coated samples, no remarkable chemical shift of the binding energy was detected in the Co 2p, Ni 2p, and Mn 2p spectra, which indicates that Co, Ni, and Mn ion environments in the structure were not affected by the coating. However, the intensities decreased implying the formation of the coating layer. Moreover, Zr 3d and F 1s spectra were clearly detected in the coated sample. The ZrF_x-coated $Li[Ni_{1/3}Co_{1/3}Mn_{1/3}]O_2$ electrode had superior electrochemical performances in comparison with the pristine electrode such as better rate capability and cyclic performance at high temperature (60 °C). The chemically vulnerable surface of the electrode was protected by the coating, which led to enhanced rate capability and cyclic performance at high temperature. The sample coated using the hydrothermal method had superior rate capability in comparison to the samples coated using the typical wet process. ZrF_x coating improved the thermal stability of the $Li[Ni_{1/3}Co_{1/3}Mn_{1/3}]O_2$ electrode as well. This demonstrates that the ZrF_x coating also effectively suppresses reactions between electrode and electrolyte in the fully charged state.

Acknowledgement

This work was supported by the Korea Research Foundation Grant funded by the Korean Government (KRF-2008-313-D00451).

References

[1] T. Ohzuku, R.J. Brodd, J. Power Sources 174 (2007) 449.
[2] J.H. Ryu, B.G. Park, S.B. Kim, Y.J. Park, J. Appl. Electrochem. 39 (2009) 1059.
[3] S.H. Yun, Y.J. Park, Bull. Korean Chem. Soc. 30 (2009) 1598.
[4] S. Beninati, L. Damen, M. Mastragostino, J. Power Sources 180 (2008) 875.
[5] Y. Koyama, N. Yabuuchi, I. Tanaka, H. Adachi, T. Ohzuku, J. Electrochem. Soc. 151 (2004) 1545.
[6] N. Yabuuchi, Y. Koyama, N. Nakayama, T. Ohzuku, J. Electrochem. Soc. 152 (2005) A1434.
[7] Y. Koyama, Y. Makimura, I. Tanaka, H. Adachi, T. Ohzuku, J. Electrochem. Soc. 151 (2004) A1499.
[8] N. Yabuuchi, Y. Makimura, T. Ohzuku, J. Electrochem. Soc. 154 (2007) A314.
[9] J. Choi, A. Manthiram, J. Electrochem. Soc. 152 (2005) A1714.
[10] K.M. Shaju, P.G. Bruce, J. Power Sources 174 (2007) 1201.
[11] S. Zhang, X. Qiu, Z. He, D. Weng, W. Zhu, J. Power Sources 153 (2006) 350.
[12] S.-T. Myung, K. Izumi, S. Komaba, Y.-K. Sun, H. Yashiro, N. Kumagai, Chem. Mater. 17 (2005) 3695.
[13] J. Cho, Y.J. Kim, T.-J. Kim, B. Park, Angew. Chem. Int. Ed. Engl. 40 (2001) 3367.
[14] J. Cho, Y.J. Kim, B. Park, Chem. Mater. 12 (2000) 3788.
[15] J. Cho, Y.J. Kim, B. Park, J. Electrochem. Soc. 148 (2001) A1110.
[16] K. Amine, H. Yasuda, M. Yamachi, Electrochem. Solid State Lett. 3 (2000) 178.
[17] M.M. Thackeray, C.S. Johnson, J.S. Kim, K.C. Lauzze, J.T. Vaughey, N. Dietz, D. Abraham, S.A. Hackney, W. Zeltner, M.A. Anderson, Electrochem. Commun. 5 (2003) 752.
[18] S.-T. Myung, K. Izumi, S. Komaba, H. Yashiro, H.J. Bang, Y.K. Sun, N. Kumagai, J. Phys. Chem. C 111 (2007) 4061.
[19] H. Lee, Y. Kim, Y.S. Hong, Y. Kim, M.G. Kim, N.-S. Shin, J. Cho, J. Electrochem. Soc. 153 (2006) A781.
[20] J. Cho, H. Kim, B. Park, J. Electrochem. Soc. 151 (2004) A1707.
[21] K.S. Ryu, S.H. Lee, B.K. Koo, J.W. Lee, K.M. Kim, Y.J. Park, J. Appl. Electrochem. 38 (2008) 1385.
[22] J. Cho, Y.-W. Kim, B. Kim, J.-G. Lee, B. Park, Angew. Chem. Int. Ed. Engl. 115 (2003) 1656.
[23] S. Lim, J. Cho, Electrochem. Commun. 10 (2008) 1478.
[24] S.-K. Hu, G.-H. Cheng, M.-Y. Cheng, B.-J. Hwang, R. Santhanam, J. Power Sources 188 (2009) 564.
[25] S.M. Lee, S. Hyoung Oh, J.P. Ahn, W.I. Cho, H. Jang, J. Power Sources 159 (2006) 1334.
[26] L. Liao, X. Wang, X. Luo, X. Wang, S. Gamboa, P.J. Sebastian, J. Power Sources 160 (2006) 657.
[27] S. Jouanneau, J.R. Dahn, J. Electrochem. Soc. 151 (2004) A1749.
[28] G.H. Kim, S.T. Myung, H.J. Bang, J. Prakash, Y.K. Sun, Electrochem, Solid State Lett. 7 (2004) A477.
[29] B.-C. Park, H.-B. Kim, S.-T. Myung, K. Amine, I. Belharouak, S.-M. Lee, Y.K. Sun, J. Power Sources 178 (2008) 826.
[30] Y.K. Sun, S.-W. Cho, S.-W. Lee, C.S. Yoon, K. Amine, J. Electrochem. Soc. 154 (2007) A168.
[31] J.M. Zheng, Z.R. Zhang, X.B. Wu, Z.X. Dong, Z. Zhu, Y. Yang, J. Electrochem. Soc. 155 (2008) A775.
[32] J.M. Bobe, J.M. Reau, J. Senegas, M. Poulain, J. Non-Cryst. Solids 209 (1997) 122.
[33] J.O. Warne, G. Hanson, J.R. Pilbrow, D.R. MacFarlane, J. Non-Cryst. Solids 140 (1992) 319.
[34] J. Mathew, R. Doremus, J. Non-Cryst. Solids 102 (1988) 165.
[35] S. Verdier, N. van der Laak, F. Dalard, J. Metson, S. Delalande, Surf. Coat. Technol. 200 (2006) 2955.